

REFINEMENT OF THE CRYSTAL STRUCTURE OF NUFFIELDITE, $\text{Pb}_2\text{Cu}_{1.4}(\text{Pb}_{0.4}\text{Bi}_{0.4}\text{Sb}_{0.2})\text{Bi}_2\text{S}_7$: STRUCTURAL RELATIONSHIPS AND GENESIS OF COMPLEX LEAD SULFOSALT STRUCTURES

YVES MOËLO¹ AND ALAIN MEERSCHAUT

*Institut des Matériaux, Laboratoire de Chimie des Solides, UMR 110 (CNRS – Université de Nantes),
2, rue de la Houssinière, B.P. 32 229, F-44322 Nantes Cedex 03, France*

EMIL MAKOVICKY

*Department of Mineralogy, Geological Institute, University of Copenhagen, Øster Voldgade 10,
DK-1350 Copenhagen K, Denmark*

ABSTRACT

A crystal-structure refinement of nuffieldite from Les Houches (France) indicates the composition $\text{Pb}_2\text{Cu}_{1.37}(\text{Pb}_{0.37}\text{Bi}_{0.39}\text{Sb}_{0.24})\text{Bi}_2\text{S}_7$. There are significant differences relative to the originally reported structure, primarily concerning the distribution of heavy atoms (Pb, Bi and Sb) and of Cu. There are two distinct Cu sites: *Cu(1)* (full occupancy) shows a pronounced eccentric tetrahedral coordination, whereas the partly occupied *Cu(2)* site has a (sub)regular tetrahedral coordination. Using the general crystal-chemical principles developed by Makovicky (1993) for complex lead sulfosalts, nuffieldite is compared with aikinite, the meneghinite homologues, berthierite and galenobismutite. The role of Cu in linking adjacent rod-layers across the incommensurate interface in the nuffieldite structure is illustrated by bond-valence calculations. The hierarchy of structural organization (from 0-D to 3-D) in complex lead sulfosalts takes into account bond valence at corresponding structural levels, and is an effective way to understand the dynamics of crystallization of such structures.

Keywords: nuffieldite, crystal structure, chemical bonding, lead sulfosalt, structural hierarchy.

SOMMAIRE

La structure cristalline de la nuffieldite a été affinée à partir d'un cristal des Houches (France), sur la base de la composition $\text{Pb}_2\text{Cu}_{1.37}(\text{Pb}_{0.37}\text{Bi}_{0.39}\text{Sb}_{0.24})\text{Bi}_2\text{S}_7$. Il apparaît des différences significatives par rapport à la structure publiée antérieurement, notamment dans la distribution des atomes lourds (Pb, Bi et Sb) et celle de Cu. Il y a deux sites à Cu: *Cu(1)*, totalement occupé, montre une coordination tétraédrique nettement excentrée, tandis que le site *Cu(2)*, partiellement occupé, est proche d'une coordination tétraédrique régulière. Sur la base des principes cristalochimiques définis par Makovicky (1993) pour les sulfosels complexes de plomb, la structure de la nuffieldite est comparée à celles de l'aikinite, des homologues de la ménégghinite, de la berthierite et de la galénobismutite. Dans la nuffieldite, la part prise par le cuivre dans la liaison entre couches colonnaires selon une interface incommensurable est estimée à partir du calcul des valences de liaison. Dans les sulfosels complexes de plomb, la hiérarchisation des niveaux d'organisation structurale (de 0 D à 3 D) peut être mieux cernée par la prise en compte des valences de liaison à chaque niveau d'organisation, et constitue une voie pour appréhender la dynamique de cristallisation de telles structures.

Mots-clés: nuffieldite, structure cristalline, liaison chimique, sulfosel de plomb, hiérarchie structurale.

INTRODUCTION

Nuffieldite is a complex Pb–Bi–Cu sulfosalt discovered by Kingston (1968) in the Lime Creek molybdenum deposit, British Columbia. Its structure was solved by Kohatsu & Wuensch (1973), with the proposed structural formula $\text{Pb}_2\text{Cu}(\text{Pb},\text{Bi})\text{Bi}_2\text{S}_7$. A second occurrence was described by Hurny & Kristin

(1978) in the Spis-Gemer Ore Mountains, Slovakia. During the study of a third occurrence from Les Houches, France, Moëlo (1989) discovered the presence of a minor amount of antimony that could explain the stabilization of this species in nature. The experimental data of Maurel & Moëlo (1990) showed that nuffieldite could only be synthesized with minor antimony. Moëlo (1989) and Maurel & Moëlo (1990)

¹ E-mail address: yves.moelo@cnsr-immn.fr

TABLE 1. ATOMIC COORDINATES FOR NUFFIELDITE

Atom	K & W	This study	x	y	(B _{eq} , B _{iso} *) Å ²	Atom	x	y	(B _{eq} , B _{iso} *) Å ²
M(1)	Pb, Bi	Pb	0.1558(1)	0.1955(1)	1.98(4)	S(1)	0.5186(8)	0.2437(5)	1.0(2)*
M(2)	Pb	Bi	0.3905(1)	0.33299(8)	1.17(3)	S(2)	0.0067(9)	0.1109(5)	1.2(2)*
M(3)	Pb	Pb	0.6326(2)	0.0239(1)	2.65(4)	S(3)	0.4429(8)	0.0634(5)	1.1(2)*
M(4)	Bi	Bi, Pb, Sb	0.6000(2)	0.4709(1)	1.61(4)	S(4)	0.8006(8)	0.2311(5)	0.9(2)*
M(5)	Bi	Bi	0.9540(1)	0.34229(9)	1.36(3)	S(5)	0.1290(8)	0.3708(5)	1.0(2)*
Cu(1)	Cu	Cu	0.6718(5)	0.1722(3)	2.0(1)*	S(6)	0.7269(9)	0.3879(6)	1.4(2)*
Cu(2)	□	0.37 Cu	0.281(1)	0.0696(8)	1.9(3)*	S(7)	0.3108(9)	0.4709(6)	1.7(2)*

Unit cell : a = 14.4949(23) Å ; b = 21.4195(49) Å ; c = 4.0420(15) Å ; V = 1254.93(95) Å³. Z = 4 ; d_{calc} = 7.046(5).

z = 1.4 for all atoms. Occupancy for M(4) = 0.39 Bi + 0.37 Pb + 0.24 Sb. K & W : Kohatsu & Wuensch (1973).

Space group: *P6mm*

pointed out the presence of excess copper relative to the crystal-structure formula, giving the general formula $Pb_2Cu_{1+x}(Pb_yBi_{1-y}Sb_z)Bi_2S_{7-y}$, with x close to 0.37, and y between 0.19 and 0.55. Re-examination of nuffieldite from the type locality and a new occurrence from Izok Lake, Northwest Territories, confirms the presence of Sb and excess Cu (Harris 1993). Similar results were obtained by Efimov *et al.* (1990) for nuffieldite from the Aktachau deposit, Kazakhstan, and by Mozgova *et al.* (1994) for nuffieldite from the Maleevskoe deposit, Russia. These last authors introduced vacancies in the sulfur sites, and proposed a new formula, $Pb_2Cu_{1+x}(Pb_yBi_{1-y}Sb_z)Bi_2S_{7-y}$.

TABLE 2. NUFFIELDITE: ANISOTROPIC DISPLACEMENT PARAMETERS FOR M ATOMS

Atom	U ₁₁	U ₂₂	U ₃₃	U ₁₂	U ₁₃	U ₂₃
M(1) = Pb	0.030(1)	0.034(1)	0.0119(7)	-0.009(1)	0	0
M(2) = Bi	0.0174(8)	0.0171(8)	0.0099(6)	0.0022(8)	0	0
M(3) = Pb	0.032(1)	0.044(1)	0.0250(9)	-0.013(1)	0	0
M(4) = (Pb, Bi, Sb)	0.022(1)	0.026(1)	0.0136(8)	0.001(1)	0	0
M(5) = Bi	0.0187(9)	0.0226(9)	0.0103(6)	0.0006(9)	0	0

The present crystal-structure study was done in order to determine the position of the excess Cu and the choice of the Bi site favored by Pb and Sb. Our findings also permit an evaluation of the validity of the two formulae given above.

CRYSTAL-STRUCTURE INVESTIGATION

Experimental

A nuffieldite needle (0.03 × 0.03 × 1.7 mm) was selected from the Les Houches deposit; its formula is $Pb_2Cu_{1.37}(Pb_{0.4}Bi_{0.47}Sb_{0.24})_{\Sigma 1.11}Bi_2S_7$, according to an electron-probe micro-analysis (Moëlo 1989). Diffraction intensities for this single crystal were collected using an ENRAF-NONIUS CAD4 diffractometer with graphite-monochromated MoK α

radiation and an $\omega/2\theta$ scan. Three reflections were measured every hour, and showed no significant change in intensity during data collection. A total of 3254 unique reflections were measured in the range $0 \leq h \leq 23$, $0 \leq k \leq 34$, $-6 \leq l \leq 0$ ($1.5^\circ \leq \theta \leq 35^\circ$). Unit-cell parameters were refined by least-squares (CELLDIM program) using 25 reflections with $15 < 2\theta < 64^\circ$. The unit cell was chosen so as to correspond to that of Kohatsu & Wuensch (1973). The intensity data

TABLE 3. NUFFIELDITE: INTERATOMIC DISTANCES IN METAL-ATOM POLYHEDRA

M(1) = Pb	M(2) = Bi	M(3) = Pb	M(4) = (Pb, Bi, Sb)
S(2) 2.817(13)	S(1) 2.663(13)	S(3) 2.876(13)	S(6) 2.555(13)
S(6) 2.888(9) x 2	S(4) 2.770(8) x 2	S(3) 2.963(9) x 2	S(7) 2.705(9) x 2
S(1) 3.120(10) x 2	S(2) 2.894(9) x 2	S(5) 3.029(9) x 2	S(2) 2.997(9) x 2
S(4) 3.310(10) x 2	S(7) 3.167(14)	S(7) 3.282(11) x 2	S(2) 3.371(12)
		S(6) 3.551(13)	
M(5) = Bi	Cu(1)	Cu(2)	
S(5) 2.607(13)	S(4) 2.251(14)	S(3) 2.351(11)	
S(3) 2.862(9) x 2	S(5) 2.308(7) x 2	S(6) 2.352(11) x 2	
S(1) 2.890(9) x 2	S(1) 2.694(14)	S(7) 2.495(23)	
S(4) 3.255(12)			
S(6) 3.432(13)			

were corrected for Lorentz-polarization effects and for absorption by an empirical method [PSI and DIFABS programs; Walker & Stuart (1983)].

Structure determination

The results of Kohatsu & Wuensch (1973) were used as a starting model. During the course of the refinement, an additional position appeared in the difference-Fourier syntheses. Introducing this new site into the refinement as a partly occupied Cu atom significantly lowered the R value.

At first, an empirical absorption based on ψ scans was applied to the data. After isotropic refinement of all atoms, a DIFABS correction was done, following which the Pb, Bi and Sb atoms were refined anisotropically. Full-matrix least-squares minimized

TABLE 4. BOND-VALENCE* TABLE FOR NUFFIELDITE

	M(1) Pb	M(2) Bi	M(3) Pb	M(4) (Pb,Bi,Sb)	M(5) Bi	Cu(1) Cu	Cu(2) 0.37 Cu	ΣV
S(1)	0.21 ^{±2}	0.74			0.40 ^{±2}	0.11		2.07
S(2)	0.49	0.40 ^{±2}		0.28 ^{±2} 0.10				1.95
S(3)			0.41 0.33 ^{±2}		0.43 ^{±2}		0.10	2.03
S(4)	0.13 ^{±2}	0.55 ^{±2}			0.15	0.35		1.86
S(5)			0.27 ^{±2}		0.86	0.30 ^{±2}		2.00
S(6)	0.40 ^{±2}		0.07	0.94	0.09		0.10 ^{±2}	2.10
S(7)		0.19	0.14 ^{±2}	0.60 ^{±2}			0.07	1.74
ΣV	1.97	2.83	1.96	2.80	2.76	1.06	0.37	13.75

*Bond-valence parameters from Brese & O'Keeffe (1991).

$\Sigma \omega (|F_o| - |F_c|)^2$ where $\omega = 4 F_o^2 / [\sigma(I)^2 + (0.03 F_o^2)^2]$, and the final cycle converged to $R = 0.059$, $R_w = 0.069$ for 1114 hkl [$I \geq 4\sigma(I)$] restricted to the range $0.1 \leq \sin\theta/\lambda \leq 0.8$, with 58 refined parameters; only one reflection ($52\bar{4}$) showed an abnormally high disagreement, and was rejected.

All calculations were done with the MOLEN package (Kay Fair 1990) installed on a VAX computer. Atomic coordinates and displacement parameters are listed in Tables 1 and 2, respectively. Interatomic distances are given in Table 3, and bond valences are given in Table 4.

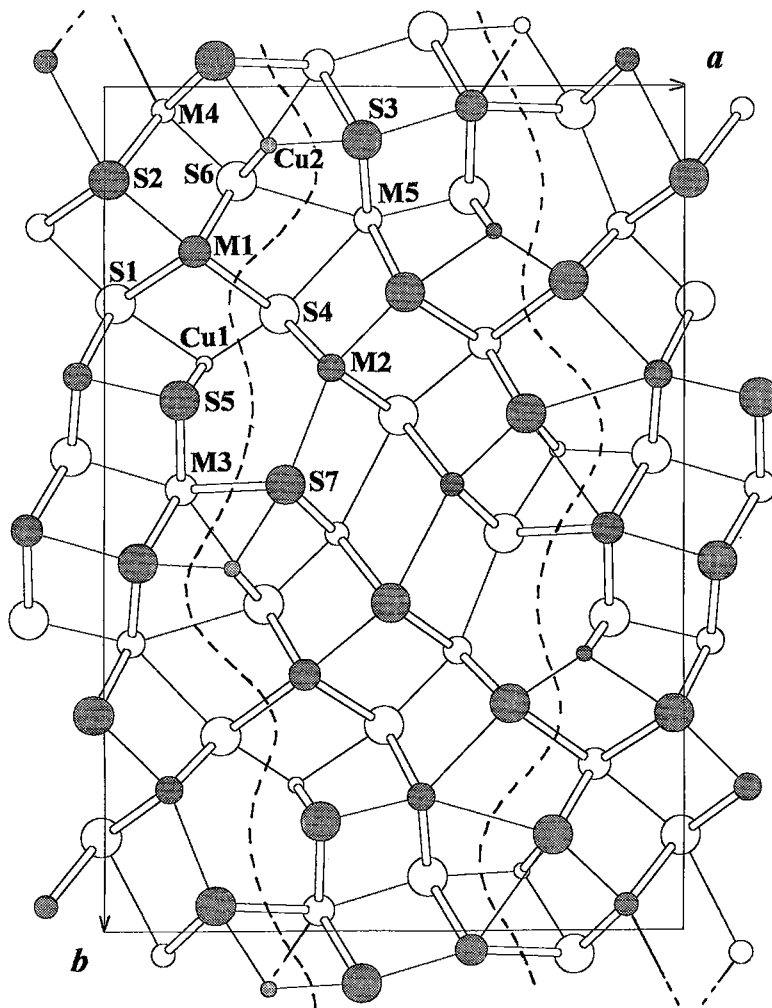


FIG. 1. Projection of the nuffeldite structure along c . Curved dashed line: incommensurate interface between two adjacent rod-layers according to the crystal-chemical principles of Makovicky (1993).

DISCUSSION OF THE STRUCTURE

Principal features and cation distribution

The general topology of the structure (Fig. 1) is the same as that determined by Kohatsu & Wuensch (1973). Besides the new site found for the excess Cu, Table 2 shows noticeable changes in the distribution of heavy cations in comparison to results of the first determination of the structure. As Pb^{2+} and Bi^{3+} are isoelectronic, the choice for Bi *versus* Pb at a given site was made according to the three shortest distances in the coordination polyhedron. Thus $M(1)$ and $M(3)$ correspond to pure Pb, whereas $M(2)$ is filled by Bi. The mixed site is $M(4)$, which contains Bi, Pb and Sb (Table 2). In cases where $M(4)$ is occupied by Sb, its lone pair of electrons will point inside the rod, approximately toward $S(7)$.

The bond valences calculated according to Brese & O'Keeffe (1991) are in good accord with the expected valences (Table 4). Nevertheless, the value for $M(4)$, which contains 0.37 Pb^{2+} , is above the expected value (2.80 *versus* 2.63 valence units, *vu*), whereas the values for pure Bi sites, $M(2)$ and $M(5)$, are slightly low. This could indicate some substitution of Pb for Bi in $M(2)$ and $M(5)$, in correlation with a lower Pb content in $M(4)$. The low bond-valence for $S(7)$ (1.74 *vu*) may reflect the complex coordination of this anion, with the mixed $M(4)$ site and the partly occupied $Cu(2)$. Any bond-valence calculation taking into account mean position(s), correlated to mixed sites, will necessarily underestimate the bond-valence relative to the effective value if one takes into account the true distribution of atoms (and vacancies) among several positions. Another question, more theoretical, is the degree of accuracy of the Brese & O'Keeffe parameters, and the limit of validity of the bond-valence model. Recently, Burdett & Hawthorne (1993) demonstrated by an orbital approach the validity of the bond-valence sum rule for regular octahedral and tetrahedral coordination geometries in oxides. Such a complex approach should be generalized, especially for covalent structures with asymmetrical coordinations due to lone pairs of electrons.

Recently, Mozgova *et al.* (1994) proposed a structural formula with sulfur vacancies that correlate with excess Cu and Pb substitution at the $M(4)$ site. According to this scheme, the vacancies would occur at the S positions connected to $Cu(2)$ and $M(4)$, that is, $S(7)$ and $S(6)$. However, any attempt to introduce vacancies at these positions did not improve the R index. Re-examination of the proposal of Mozgova *et al.* (1994) revealed an error. In the general formula $Cu_{1+x}Pb_{2+x}(Bi,Sb)_{3-x}S_7$, the atom total is $(13+x)$. If the sum is fixed at 13 atoms, as in Table 3 of Mozgova *et al.* (1994), each coefficient in the above formula must be multiplied by $13/(13+x)$. Then, in their Figure 2, the S content X equals $7 \cdot [13/(13+x)]$, and, for the

other axis, one has Pb_{mix} (*i.e.*, Pb atomic content minus 2 atoms) equal to $[(2+x) \cdot (13/(13+x))] - 2$, *i.e.*, $11x/(13+x)$ ($= Y$). Similarly, Cu_{exc} (Cu atomic content minus one atom) equals $[(1+x) \cdot (13/(13+x))] - 1 = 12x/(13+x)$ ($= Y'$). Thus Figures 2a and 2b of Mozgova *et al.* (1994) must be compared to the functions $Y = 11(1 - X/7)$ and $Y' = 12(1 - X/7)$. These functions correspond to straight lines through $X = 7$, $Y = Y' = 0$, with slopes -1.57 and -1.71 , respectively. Analytical data are in accord with these ideal correlations, and verify the above formula. The negative slopes obtained by plotting Pb_{mix} and Cu_{exc} *versus* S (Mozgova *et al.* 1994) are an artifact of calculation, and do not prove the presence of S vacancies. Our crystal-structure and electron-microprobe data exclude significant vacancies in the sulfur sites of nuffieldite.

Coordination of copper

The two Cu sites have distinct coordination geometries (Table 5). Variation in coordination geometry may be expressed in bond-valence form by taking into account the three and four closest S neighbors ($\Sigma 3$ and $\Sigma 4$ of Table 5). Data for regular tetrahedral and subregular triangular Cu-sites in tetrahedrite (Wuensch 1964) and its Cu-rich synthetic equivalent ($Cu_{13.8}Sb_4S_{13}$; Makovicky & Skinner 1979) are given as Tr and Tt in Figures 2a and 2b. The Tr-Tt segment, divided in three equal parts by four straight lines originating from $\Sigma 3 = \Sigma 4 = 0$, permits definition of three subfields corresponding to (sub)regular tetrahedra (RTT), eccentric tetrahedra (ETT) and eccentric triangles (ETR) with increasing $\Sigma 3$ and $\Sigma 4/\Sigma 3$ ratio.

The $Cu(1)$ site in nuffieldite corresponds to an eccentric tetrahedral coordination (ETT subfield:

TABLE 5. BOND-VALENCE SUM (ν_b) FOR THE THREE ($\Sigma 3$) AND FOUR ($\Sigma 4$) CLOSEST S ATOMS AROUND Cu ATOMS IN NUFFIELDITE AND VARIOUS SULFOSALTS OF Pb

Sulfosalt	Reference	n° Cu *	$\Sigma 3$	$\Sigma 4$
- a -				
Seligmannite	Takéuchi & Haga (1969)		0.852	1.091
Seligmannite	Edenharter <i>et al.</i> (1970)		0.893	1.139
Bourmonite	Edenharter <i>et al.</i> (1970)		0.867	1.112
Aikinite	Ohmura & Nowacki (1970)		0.828	1.061
Aikinite	Kohatsu & Wuensch (1971)		0.800	1.015
Hammarite	Horiuchi & Wuensch (1976)	Cu 1	0.939	1.198
		Cu 2	0.737	0.945
			0.784	1.043
Lindströmite	Kaplunuk <i>et al.</i> (1975)		0.805	1.044
Krupkajte	Mumme (1975a)	Cu 1 (20)	0.866	1.105
		Cu 2 (80)	0.899	1.054
Gladite	Kohatsu & Wuensch (1976)		0.874	1.154
Pekoite	Mumme & Watts (1976)			
- b -				
Jaskolskiite	Makovicky & Nørrestam (1985)	(20)	0.753	0.980
Izoklakeite	Makovicky & Mumme (1986)	(Cu,Fe)	0.982	1.125
Izoklakeite (Bi-rich)	Armbruster & Hummel (1987)	(Cu,Fe)	0.859	1.111
Kobellite	Miehe (1971)	(Cu,Fe)	0.859	1.092
Eclairite	Kupčik (1984)	(Cu,Fe)	0.828	1.054
Coosalite	Srikrishnan & Nowacki (1974)	(12)	0.714	0.846
Nuffieldite	This study	Cu(1)	0.941	1.047
		Cu(2) (37)	0.798	0.975
			0.858	1.026
Junoite	Mumme (1975b)			
- Standard -				
Tetrahedrite	Wuensch (1964)	Cu triang.	1.021	1.021
		Cu tetra.	0.815	1.087
		Cu triang.	1.011	1.011
		Cu tetra.	0.792	1.056
Cu-rich tetrahedrite (synth.)	Makovicky & Skinner (1979)			

*: if distinct Cu sites. (x) = partial occupancy (in %)

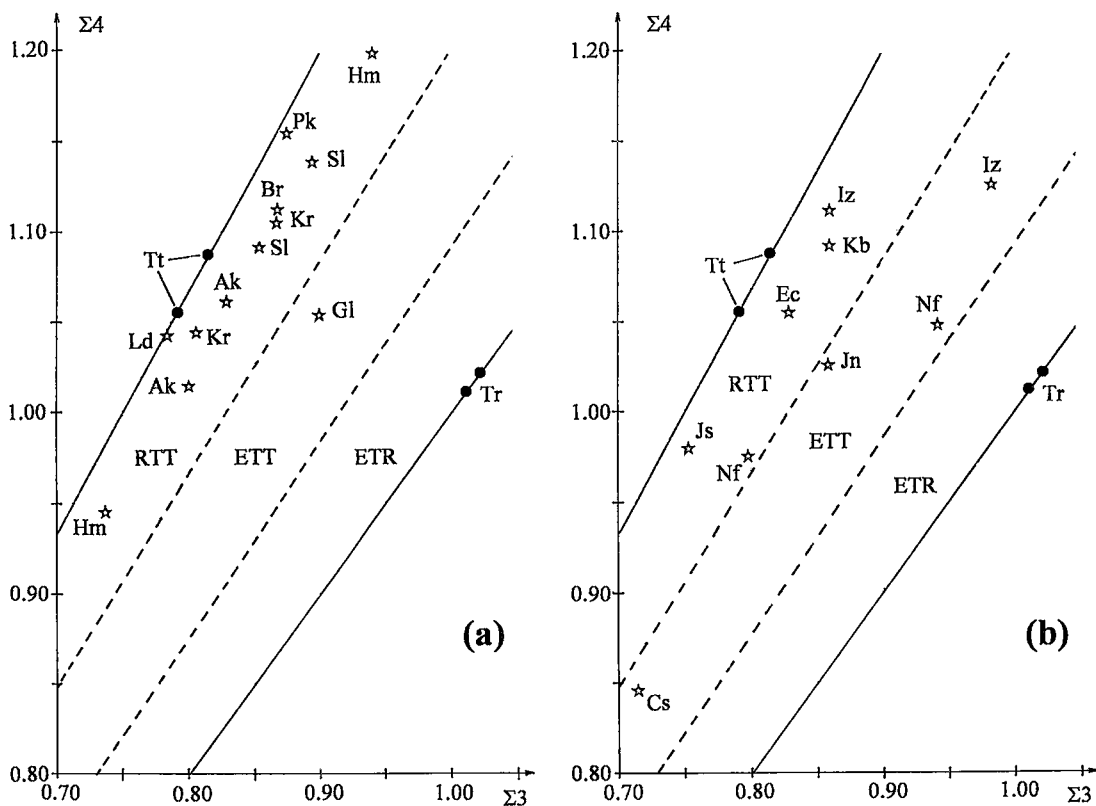


FIG 2. Bond-valence diagram for Cu in Cu-Pb-Bi-(Sb, As) sulfosalts. Correlation between bond-valence sums of the four closest S neighbors ($\Sigma 4$) and of the three closest ones ($\Sigma 3$), according to the data quoted in Table 6. a: Selected Cu-rich Pb sulfosalts (Br: bournonite, Sl: seligmannite, Ak: aikinite, Hm: hammarite, Ld: lindströmite, Kr: krupkaite, Gl: gladite, Pk: pekoite). b. Nuffieldite (Nf) and Cu-poor Pb sulfosalts (Js: jaskólskiite, Iz: izoklakeite, Kb: kobellite, Ec: eclarite, Cs: cosalite, Jn: junosite). Tt and Tr: regular tetrahedral and triangular coordinations in tetrahedrite. RTT, ETT and ETR: fields of regular tetrahedral, eccentric tetrahedral and eccentric triangular coordinations, respectively.

Fig. 2b). The Cu(2) site is tetrahedrally coordinated, with a small eccentricity of the Cu atom (RTT subfield: Fig. 2b). For comparison, numerous Cu-rich and Cu-poor Pb sulfosalts have been considered (Table 5a and b, respectively). Cu-rich Pb sulfosalts have close to ideal Cu coordination (RTT subfield: Fig. 2a), with the exception of gladite (ETT subfield). The variation is more extensive for Cu-poor Pb sulfosalts (Fig. 2b). One must point out that for all these Pb-sulfosalts, the average incident bond-valence around Cu ($\Sigma 4$) is 1.05, slightly higher than the ideal value of 1.0. This discrepancy may result from an overestimation of the Cu-S bond-valence parameter (1.86) given by Brese & O'Keeffe (1991); a better fit is obtained with the value 1.84.

Role of copper in inter-layer bonding

In nuffieldite, Cu plays an important role in connecting adjacent rod-layers. According to Makovicky (1981, 1985), the nuffieldite structure is composed of two types of rods; one rod is of the aikinite-bismuthinite type (defined by Kohatsu & Wuensch 1973), the other is the M_6S_{10} rod, corresponding to a rod of distorted PbS structure, transitional to SnS. Each rod-layer parallel to the (b, c) plane consists of a regular alternation of these two types of rods, connected via the S(1) atom.

Perpendicular to (100), connection between adjacent rod-layers is reinforced by Cu atoms in two ways. First, the eccentric tetrahedral coordination of

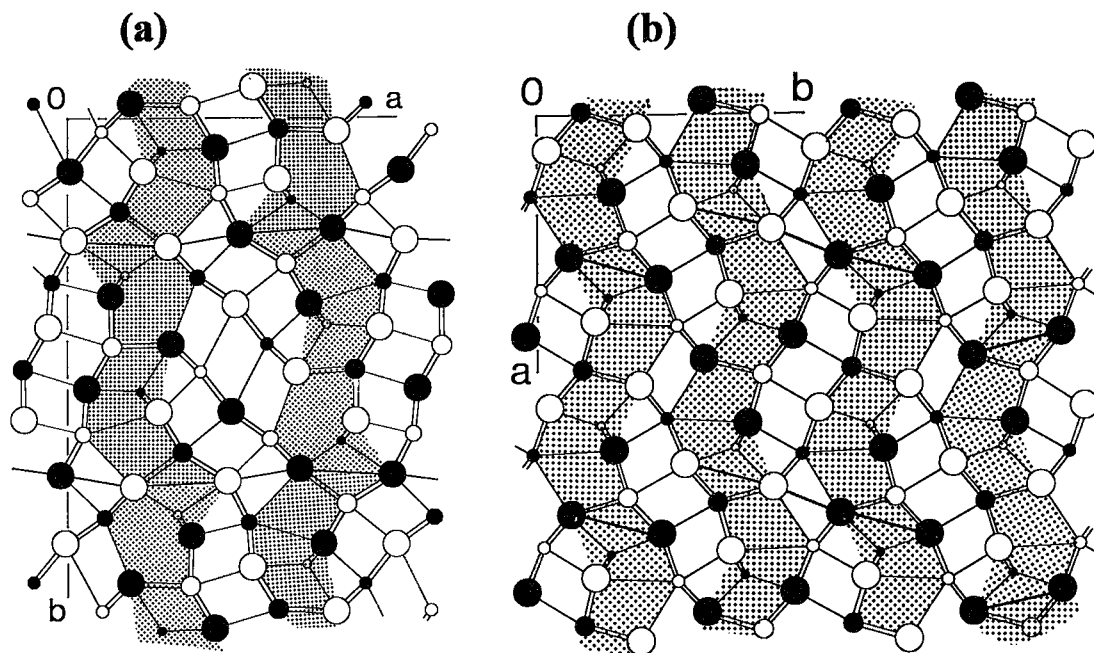


FIG. 3. Comparison of interfaces in nuffieldite (a) and aikinite (b). Interfaces are stippled, planes of reversal for adjacent intervals are indicated by heavy solid lines. Alternative choices of these planes in aikinite are indicated. Filled and void circles represent two atomic levels 2 Å apart.

the Cu(1) atom weakens its bonding with the S(1) atom of a M_6S_{10} rod from the same rod-layer, and reinforces the connection between an aikinite-type rod [two bonds to the S(5) atom] and an M_6S_{10} rod of the adjacent rod-layer through a bond to the S(4) atom. Furthermore, the Cu(2) site interconnects S(3) of the aikinite-type rod and S(6) and S(7) of the M_6S_{10} rod. Thus, the S(1) atoms organize a two-dimensional rod-layer structure parallel to (100), whereas the three-dimensional organization is provided by Cu–S bonding, plus weak Pb–S or Bi–S bonding between these layers. Occupancy of the M(1) and M(3) sites by Pb only agrees better with the specific crystal-chemical role of Pb in providing the connection between rod-layers *via* an incommensurate interface (Makovicky 1993) than the model with mixed (Pb, Bi) on M(1) proposed by Kohatsu & Wuensch (1973).

The zig-zag incommensurate interface (Fig. 1) cuts specific Cu–S and M–S bonds. The ratio of the total bond-valence of these bridging bonds to the total bond-valence of the Cu and M cations involved is a measure of the interface bonding. For one formula unit, the bond-valence across the interface is 0.45 *vu* for Cu–S bonds and 0.77 *vu* for M–S bonds (total: 1.22 *vu*). The total bond-valence of the cations involved is 11.37 *vu*, giving a ratio 1.22/11.37 = 11%. Cu–S interface bonding participates for about 37% (= 0.45/1.22) of the

total interface bonding, which illustrates the important role of interstitial copper in linking adjacent rod-layers.

COMPARISON WITH OTHER SULFOSALT STRUCTURES

Nuffieldite cannot be classified as a member of any of the extensive homologous series in the sulfosalt minerals. However, it shows features akin to a number of distinct structure-types. The following relationships will be discussed: (1) to aikinite, (2) to other meneghinite homologues and berthierite, (3) to sheared noncommensurate sandwich-type compounds, as represented by the weibullite–galenobismutite pair, (4) to galenobismutite-related rod-packing plesiotypes.

Comparison with aikinite

Relations to aikinite, *i.e.*, to a structure with a common type of ribbon, were noted by Kohatsu & Wuensch (1973). Those intervals of the rod-layer interface between two consecutive S(1) and S(4) positions along [001] of nuffieldite are identical to the corresponding periodically repeated intervals in aikinite (Figs. 3a, b). On every S(1)–S(4) boundary, the interface in nuffieldite is reversed relative to that in aikinite (Fig. 3). The planes of reversal, S(1)–S(4)–S(1)–S(4), are

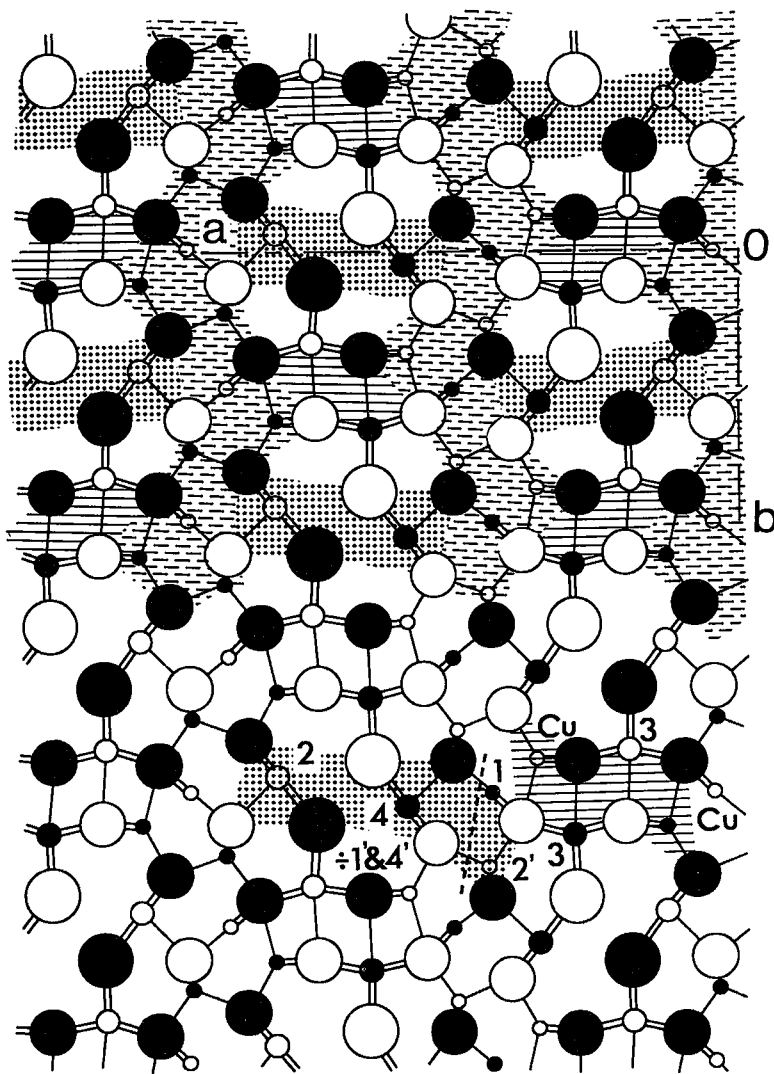


FIG. 4. The crystal structure of $\text{Bi}_2\text{Cu}_3\text{S}_4\text{Cl}$ (Lewis & Kupčik 1974) interpreted as a sheared, SnS -based sandwich structure with broad Cu -occupied boundaries shearing the H (ruled) and Q (stippled) stacks of layers. Relation of its Q and H rods to those in nuffieldite is shown below (designations of cations show the corresponding numbers in nuffieldite; vertical 2 \AA shear is indicated by a dashed line).

continuous (001) planes in nuffieldite. The corresponding planes in aikinite are without reversal, and are broken into glide- or rotation-related fragments, inclined with respect to (001) of aikinite. These fragments represent individual "S(1)–S(4)–S(1)–S(4)" intervals when the nuffieldite notation is used. As a corollary, these two compounds are not even partial polytypes, and the angles comprised by the aikinite ribbons and the glide planes in the rod-layer interface differ between

these structures. The thickness of rod-like elements in these structures is directly related to the presence or absence of interface reversals.

Comparison with meneghinite homologues

The truncated rods $M_6\text{S}_{10}$ (this formula disregards S-sharing with adjacent ribbons) can be interpreted as fragments of the meneghinite homologue $N = 3$ [here N

is equal to the number of square pyramids defining the width of a layer (or rod) in a homologous series], which has not yet been found as a complete structure. In all meneghinite homologues, the layer interfaces being identical with the interface in the bismuthinite–aikinite solid-solution series (Makovicky 1985), the above conclusions about interfaces are valid for $N = 3$ as well. The same rod fragments can be derived from the structure of berthierite (Buerger & Hahn 1955), but the interfaces in berthierite (involving half-octahedra of Fe) are not those in nuffieldite. In nuffieldite, the chess-board intergrowth of fragments from a meneghinite homologue $N = 2$ (aikinite-like ribbons) with the fragments from the homologue $N = 3$ (M_6S_{10} rods) does not sum to a meneghinite-like composite $N = 2,3,2,3$. These types of elements are oriented with much more and much less acute angles, respectively, to the interface glide-plane than in a real meneghinite homologue. The rod-layer in nuffieldite (Fig. 5d) is rather close to the thinner composite rod-layer in $Sn_6Sb_{10}S_{21}$ (Fig. 5f; Parise & Smith 1984). Differences occur both in the archetype and its orientation for the rod-like elements, and in the looser attachment of the aikinite-like ribbon (*via* a lone-pair electron interface) to the rods in $Sn_6Sb_{10}S_{21}$.

Comparison with sheared noncommensurate sandwich compounds

In spite of its meneghinite-series connections, nuffieldite fits best into the plesiotypic family (Makovicky 1994) of sheared noncommensurate sandwich structures. This family has (single- or double-) layers of octahedra [undeformed or deformed (111)_{PbS} slabs: *H* type] alternating with square pyramidal layers [(100)_{PbS} slabs two atomic planes thick: *Q* type] in noncommensurate contact with each other (*Q/H* interface). This internally noncommensurate stack of layers is periodically sheared by out-of-phase boundaries that are compositionally non-conservative. For plesiotypes closest to nuffieldite, these out-of-phase boundaries are perpendicular to the *H* and *Q* layers and are glide-planes displacing these layer sets. The width of these boundaries varies from one layer of S atoms (in nuffieldite) to two coordination polyhedra in $CeTmS_3$ (Rodier 1973) (Table 6).

Within this plesiotypic family, nuffieldite shows the closest relation to $Cu_2Bi_3S_4Hal$ (Hal: Cl, Br) (Lewis & Kupčik 1974, Mariolacos & Kupčik 1975). In this structure (Fig. 4), the aikinite-like ribbons ($N = 2$) from nuffieldite are reduced to columns of paired square-pyramids of Bi ($N = 1$). These pyramids are flanked by Cu tetrahedra exactly as in nuffieldite. The M_6S_{10} rods of nuffieldite are reduced to a single layer of octahedra [the positions preserved, numbers 2 and 4 of Fig. 4, correspond to $M(4)$ and $M(2)$ of nuffieldite at one of the interfaces]. The octahedra are very deformed and resemble a pure SnS-archetype. The

TABLE 6. SHEARED NONCOMMENSURATE SANDWICH SULFIDE STRUCTURES

Mineral or phase	Structural formula	Lattice parameters (Å and degr.)				Space group	References
		Layer stack	Shear. direct.	Short period	Angle in layers		
Weibullite	$Ag_{0.13}Pb_{1.23}Bi_{4.53}(S,Se)_{18}$	c 15.42	a 53.68	b 4.11		<i>Pnma</i>	Mumme (1980)
Galenobismutite	$PbBi_3S_4$	b 14.59	a 11.79	c 4.10		<i>Pnma</i>	Iitaka & Nowacki (1962)
Synth.	$CeTmS_3$	a 11.09	b 21.42	c 3.98	γ 102.9	<i>P2₁/m</i>	Rodier (1973)
Nuffieldite	$Pb_2Cu_{1.37}(Pb_{0.40}Bi_{0.47}Sb_{0.21})Bi_3S_7$	b 14.49	c 21.42	a 4.04		<i>Pbmm</i>	This study
Synth.	$Bi_3Cu_3S_4Cl$	b 10.31	a 20.72	c 4.00		<i>P2₁2₁2₁</i>	Lewis & Kupčik (1974)
Synth.	$Bi_3Cu_3S_4Br$	b 10.44	a 20.93	c 4.02		<i>P2₁2₁2₁</i>	Mariolacos & Kupčik (1975)

adjacent polyhedra [$M(1)$ of nuffieldite] and the $M(2)$ polyhedra from the adjacent layer of octahedra of the same rod of nuffieldite, underwent 2 \AA shear (along the 4 \AA axis) and deformation; now they host triangularly and tetrahedrally coordinated Cu, respectively (numbers 1 and 2' of Fig. 4). Thus, the rod-layers in $Cu_2Bi_3S_4Hal$ differ from those in nuffieldite: (1) Crystallographic shear occurs on flanks of (now single, not double) pseudo-octahedral (SnS-like) rods; $Cu1$ and $Cu2'$ (Fig. 4) replace large cations in the sheared polyhedra. (2) Attachment of eccentric tetrahedrally coordinated Cu (identical in both structures) occurs not to the blunt edge of the SnS-like rod [*i.e.*, to the analogue of the $S(4)$ position of nuffieldite], but to the central S position of this rod [$S(7)$ of nuffieldite]. This change results from the altered fit, as the width of the (010)-rod face was preserved, whereas the aikinite ribbons were reduced to one half of the original width.

As a consequence of (1) and (2), the interface that shears and displaces (by glide-reflection) the *H/Q* layer packets is only a layer of S atoms in nuffieldite, whereas in $Cu_2Bi_3S_4Hal$, it is $\sim 3 \text{ \AA}$ thick and incorporates all Cu atoms in the apical, sheared polyhedra of the rods.

Comparison with galenobismutite

Galenobismutite $PbBi_3S_4$ (Iitaka & Nowacki 1962) is also a structure that shows kinships in several directions. It forms a homologous pair with weibullite (Mumme 1980). Another such pair, based on a different type of homologous expansion, was recognized by Makovicky (1992), and involves $Pb_4In_3Bi_7S_{18}$ (Krämer & Reis 1986). Galenobismutite has rods identical to those in Gd_3S_3 (Makovicky 1992); this mineral can also be re-interpreted as packing of the corner-sharing M_6S_{10} rods in nuffieldite, with a 2-\AA shift for two apical S atoms. In the (100) slabs of galenobismutite, these [001] rods are separated by spaces, one half of a square pyramid wide (Fig. 5a). Nuffieldite is an exploded version of such rod packing, with the spaces augmented by a combined width of two additional square pyramids and a Cu polyhedron of the aikinite-like ribbon (Fig. 5b). As a consequence, rods are separated from each other (Fig. 5c).

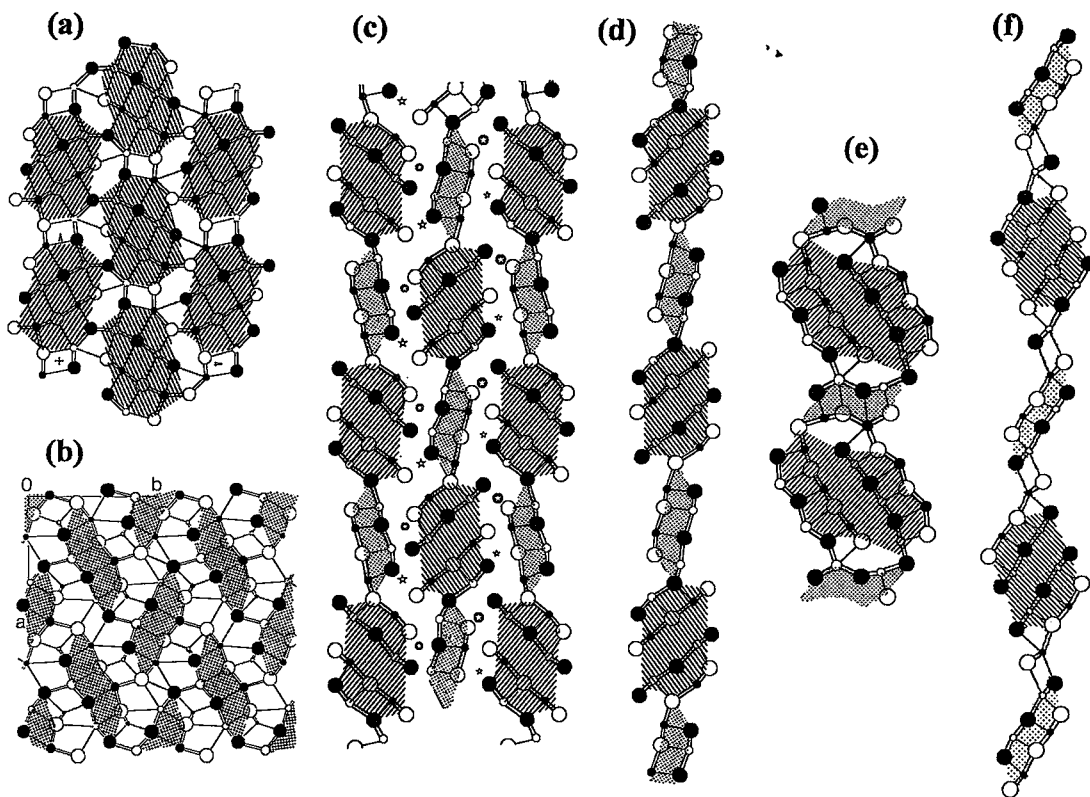


Fig. 5. Comparison between crystal structures of nuffieldite and other complex sulfides: (a) galenobismutite, (b) aikinite, (c) representation of nuffieldite structure as a chess-board intergrowth of unit rods of galenobismutite and aikinite. Similarities also exist between (d) the basic rod-layer of nuffieldite and those of (e) $\text{Eu}_3\text{Sb}_4\text{S}_9$ (compressed along a) and (f) $\text{Sn}_6\text{Sb}_{10}\text{S}_{21}$ (one of the two constituent rod-layers).

There is a close analogy between this interpretation of nuffieldite and the structure of CsBi_3S_5 (Kanishcheva *et al.* 1980, Fig. 6). In CsBi_3S_5 , the $M_6\text{S}_{10}$ rods are placed in the same chess-board pattern as in nuffieldite, but the structure has a 2 \AA shear in the $[010]$ direction, so that contact of nearest rods takes place *via* octahedral coordinations of Bi rather than trigonal prismatic coordinations of $M(1)$. The aikinite ribbons are replaced by two very large coordination polyhedra of Cs.

$M_{10}\text{S}_{14}$ rods (S sharing by rods and ribbons not taken into account) of $\text{Eu}_3\text{Sb}_4\text{S}_9$ (Lemoine *et al.* 1981, Fig. 5e) are a superficially similar, expanded version of rods previously considered; these rods are parallel to $[010]_{\text{SnS}}$ (Makovicky 1985). The aikinite-like ribbons can also be interpreted as $N = 3$; in the $N = 2$ interpretation (Fig. 5e), the ribbons are attached to the same sites of rods as in nuffieldite. The final geometry of an individual rod-layer appears compressed in a zig-zag fashion along a .

HIERARCHY OF STRUCTURAL ORGANIZATION: THE GENESIS OF COMPLEX SULFOSALT STRUCTURES

The hierarchical construction of complex crystal structures of sulfides and sulfosalts through various levels of organization (Makovicky 1994) is not only a geometrical operation. It illustrates the probable building dynamics of such structures according to the model discussed by Mořlo (1983) for Pb–Sb sulfosalts. This model is based on the principle of *condensation of intermediate substructural units*. The *first* level of condensation is the formation of complex ions, like those known for Sb with S (Brookins 1972) in hydrothermal solutions (0-D or cluster organization). The *second* level, easily recognized in the structures studied, is the formation of individual rods of various types, according to the chemical composition of the system and the intensive parameters [*e.g.*, T , $f(\text{S}_2)$] (1-D or nematic organization). The *third* level is the constitution of individual rod-layers (or other types of layers), by

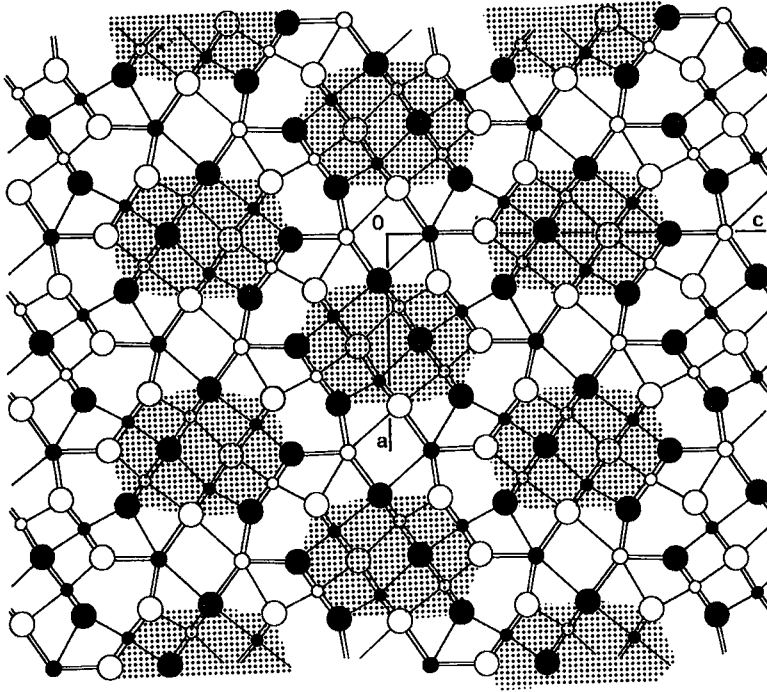


FIG. 6. The crystal structure of CsBi_3S_5 (Kanishcheva *et al.* 1980) with the stippled rods analogous to the rods in nuffieldite. In order of decreasing size, circles represent S, Cs and Bi.

condensation of one or two types of rods present in the medium of crystallization (2-D or smectic organization). In the group of rod-layer sulfosalts, various types of rod-layers can coexist at this step. Finally, the competition between coexisting rod-layer types is submitted to the rules of (a) electroneutrality and (b) of accommodation between *Q*- and *H*-type mono-atomic layers constituting the surface of a given rod-layer (Makovicky 1993). Only combinations of rod-layers of one or two types that permit such an accommodation will give a stable crystal structure (3-D organization). Competition between stable structures will give the final phase-equilibrium in a given system.

Except for the crystallization sequence from liquid to solid through a liquid crystal state (known for organic compounds), this strict distinction between successive steps of crystallization is excessive, especially at low temperatures. Very probably, the final steps do not act in free space (condensation of independent 1-D or 2-D units), but would grow in place at the expense of very small fragments (from poorly organized precipitates, or through surface processes like epitactic nucleation).

This model of crystallization dynamics is corroborated by the fact that the aikinite series and

galenobismutite, each containing one of the two basic rods of the nuffieldite structure, coexist in equilibrium with that sulfosalts. The relative positions of these species in the simplified system $\text{PbS}-\text{Sb}_2\text{S}_3-\text{Bi}_2\text{S}_3$ (see Fig. 6 of Moëlo *et al.* 1995) is in accord with the general evolution of crystal-structure subtypes with $\text{Pb}/(\text{Pb} + \text{Sb} + \text{Bi})$ and $\text{Bi}/(\text{Bi} + \text{Sb})$ values. Moreover, an interesting problem is the competition between nuffieldite and the synthetic phase AG, chemically very close to nuffieldite but without antimony (Mariolacos 1979); note that Marcoux *et al.* (1996) reported a probable natural occurrence of AG at Algaré, Spain. Without Sb and excess Cu, nuffieldite would plot exactly between aikinite and galenobismutite in the system $\text{PbS}-\text{Cu}_2\text{S}-\text{Bi}_2\text{S}_3$, but paradoxically, AG is the stable phase. Thus, it seems necessary to solve the structure of this synthetic phase to understand the relative stability of AG and nuffieldite.

CONCLUSIONS

The refinement of the crystal structure of nuffieldite has made it possible to locate the excess Cu shown by electron-microprobe analysis, and to identify the site that contains the minor Sb. More generally, it gives a

crystal-chemical formula that delimits more precisely the solid-solution field of natural and synthetic nuffieldite according to the excess Cu and Sb-for-Bi substitution. Bond-valence calculations are useful not only to illustrate the geometry of the Cu sites (position between regular tetrahedral and planar-triangular coordinations), but also to estimate the role of Cu in linking adjacent rod-layers.

Nuffieldite is transitional between sulfosalts related to the PbS archetype (e.g., galenobismutite), and to the SnS archetype (e.g., the meneghinite homologues and berthierite). In this way, it conforms to general structural trends in phase diagrams for complex sulfides. We deem it very useful to generalize the analysis of the 2-D – 3-D character performed here for nuffieldite to other structures with a complicated 2-D organization, define a degree of interlayer bonding in them, and classify these structures as intermediate between true 2-D and 3-D types of structures. In this way, we expect to develop and quantify the concept of non-integer dimensionality between the ideal 3-D and 2-D bonding schemes, but also, more generally, between pure 3-D and 0-D schemes of bonding.

ACKNOWLEDGEMENTS

We sincerely thank an anonymous reviewer and Associate Editor Frank Hawthorne for their careful reading of this manuscript, and for numerous improvements in the presentation and discussion of our structural data.

REFERENCES

- ARMBRUSTER, T. & HUMMEL, W. (1987): (Sb,Bi,Pb) ordering in sulfosalts: crystal-structure refinement of a Bi-rich izoklakeite. *Am. Mineral.* **72**, 821-831.
- BRESE, N.E. & O'KEEFE, M. (1991): Bond-valence parameters for solids. *Acta Crystallogr.* **B47**, 192-197.
- BROOKINS, D.G. (1972): Stability of stibnite, metastibnite, and some probable dissolved antimony species at 298.15°K and 1 atmosphere. *Econ. Geol.* **67**, 369-372.
- BUERGER, M.J. & HAHN, T. (1955): The crystal structure of berthierite, FeSb₂S₄. *Am. Mineral.* **40**, 226-238.
- BURDETT, J.K. & HAWTHORNE, F.C. (1993): An orbital approach to the theory of bond valence. *Am. Mineral.* **78**, 884-892.
- EDNHARTER, A., NOWACKI, W. & TAKÉUCHI, Y. (1970): Verfeinerung der Kristallstruktur von Bournonit [(SbS₃)₂][Cu₂^{IV}Pb^{VIII}Pb^{VIII}] und von Seligmannit [(AsS₃)₂][Cu₂^{IV}Pb^{VIII}Pb^{VIII}]. *Z. Kristallogr.* **131**, 397-417.
- EFIMOV, A.V., BORODAEV, YU. S., MOZGOVA, N.N. & NENASHEVA, S.N. (1990): Noteworthy Bi ore of Akchatau Mo-W deposit (central Kazakhstan). *Geol. Rud. Mest.* **4**, 64-75 (in Russ.).
- HARRIS, D.C. (1993): Confirmation of antimony in co-type nuffieldite, Lime Creek, British Columbia, and a second Canadian occurrence at Izok Lake, Northwest Territories. *Geol. Surv. Can., Pap.* **93-1E**, 9-10.
- HORIUCHI, H. & WUENSCH, B.J. (1976): The ordering scheme for metal atoms in the crystal structure of hammarite, Cu₂Pb₂Bi₄S₉. *Can. Mineral.* **14**, 536-539.
- HURNY, J. & KRISTIN, J. (1978): Chemical composition of bismuth minerals from some deposits of the northern part of the Spišsko-Gemerske Rudohorie Mountains (eastern Slovakia). *Int. Mineral. Assoc., XIth General Meet. (Novosibirsk), Abstr. Vol.*, 142.
- ITAKA, Y. & NOWACKI, W. (1962): A redetermination of the crystal structure of galenobismutite, PbBi₂S₄. *Acta Crystallogr.* **15**, 691-698.
- KANISHCHEVA, A.S., MIKHAILOV, YU. N., LAZAREV, B.V. & TRIPPEL, A.F. (1980): A new cesium sulfobismuthite: synthesis and structure containing extensive channels. *Sov. Phys. Dokl.* **25**(5), 319-320.
- KAPLUNNIK, L.N., POBEDIMSKAYA, E.A. & BELOV, N.V. (1975): The crystal structure of lindströmite, CuPbBi₃S₆. *Sov. Phys. Crystallogr.* **20**, 634-636.
- KAY FAIR, C. (1990): *MOLEN structure determination package*. Enraf-Nonius, Delft, The Netherlands.
- KINGSTON, P.W. (1968): Studies of mineral sulphosalts. XXI. Nuffieldite, a new species. *Can. Mineral.* **9**, 439-452.
- KOHATSU, I. & WUENSCH, B.J. (1971): The crystal structure of aikinite, PbCuBiS₃. *Acta Crystallogr.* **B27**, 1245-1252.
- _____ & _____ (1973): The crystal structure of nuffieldite, Pb₂Cu(Pb,Bi)Bi₂S₇. *Z. Kristallogr.* **138**, 343-365.
- _____ & _____ (1976): The crystal structure of gladite, PbCuBi₂S₉, a superstructure intermediate in the series Bi₂S₃-PbCuBiS₃ (bismuthinite – aikinite). *Acta Crystallogr.* **B32**, 2401-2409.
- KRÄMER, V. & REIS, I. (1986): Lead indium bismuth chalcogenides. II. Structure of Pb₄In₃Bi₇S₁₈. *Acta Crystallogr.* **C42**, 249-251.
- KUPČIK, V. (1984): Die Kristallstruktur des Minerals Eclarit, (Cu,Fe)Pb₃Bi₁₂S₂₈. *Tschermaks Mineral. Petrogr. Mitt.* **32**, 259-269.
- LEMOINE, P., CARRÉ, D. & GUITTARD, M. (1981): Structure du sulfure d'europium et d'antimoine, Eu₃Sb₄S₉. *Acta Crystallogr.* **B37**, 1281-1284.
- LEWIS, J., JR. & KUPČIK, V. (1974): The crystal structure of Bi₂Cu₃S₄Cl. *Acta Crystallogr.* **B30**, 848-852.
- MAKOVICKY, E. (1981): The building principles and classification of bismuth-lead sulphosalts and related compounds. *Fortschr. Mineral.* **59**, 137-190.

- _____ (1985): The building principles and classification of sulphosalts based on the SnS archetype. *Fortschr. Mineral.* **63**, 45-89.
- _____ (1992): Crystal chemistry of complex sulfides (sulphosalts) and its chemical application. In *Modern Perspectives in Inorganic Crystal Chemistry* (E. Parthé, ed.). Kluwer, Dordrecht, The Netherlands (131-161).
- _____ (1993): Rod-based sulphosalts structures derived from the SnS and PbS archetypes. *Eur. J. Mineral.* **5**, 545-591.
- _____ (1994): Modular classification of complex sulfides. *Int. Mineral. Assoc., XVIIth General Meet. (Pisa), Abstr. Vol.*, 256-257.
- _____ & MUMME, W.G. (1986): The crystal structure of izoklakeite, $Pb_{51.3}Sb_{20.4}Bi_{19.5}Ag_{1.2}Cu_{2.9}Fe_{0.7}S_{114}$. The kobellite homologous series and its derivatives. *Neues Jahrb. Mineral., Abh.* **153**, 121-145.
- _____ & NØRRESTAM, R. (1985): The crystal structure of jaskolskiite, $Cu_xPb_{2-x}(Sb,Bi)_{2-x}S_5$ ($x \approx 0.2$), a member of the meneghinite homologous series. *Z. Kristallogr.* **171**, 179-194.
- _____ & SKINNER, B.J. (1979): Studies of the sulphosalts of copper. VII. Crystal structures of the exsolution products $Cu_{12.3}Sb_4S_{13}$ and $Cu_{13.8}Sb_4S_{13}$ of unsubstituted synthetic tetrahedrite. *Can. Mineral.* **17**, 619-634.
- MARCOUX, E., MOËLO, Y. & LEISTEL, J.M. (1996): Bismuth and cobalt minerals as indicators of stringer zones to massive sulphide deposits, Iberian Pyrite Belt. *Mineral. Deposita* **31**, 1-26.
- MARIOLACOS, K. (1979): Phase relations in the system Bi_2S_3 -PbS-CuPbBiS₃ at 450°C and its extension in the system Bi_2S_3 -PbS-Cu₂S. *Neues Jahrb. Mineral., Monatsh.*, 73-80.
- _____ & KUPČIK, V. (1975): Die Kristallstruktur des $Bi_2Cu_3S_4Br$. *Acta Crystallogr.* **B31**, 1762-1763.
- MAUREL, C. & MOËLO, Y. (1990): Synthèse de la nuffieldite dans le système Bi-Pb-Sb-Cu-S. *Can. Mineral.* **28**, 745-749.
- MIEHE, G. (1971): Crystal structure of kobellite. *Nature Phys. Sci.* **231**, 133-134.
- MOËLO, Y. (1983): Contribution à l'étude des conditions naturelles de formation des sulfures complexes d'antimoine et plomb. *Bur. Rech. Géol. Minières (Orléans, France), Doc.* **55**.
- _____ (1989): Antimoine dans la nuffieldite associée à de la friedrichite (commune des Houches, Alpes de Haute-Savoie); redéfinition cristallographique de la nuffieldite. *C. R. Acad. Sci. Paris* **309**, Sér. II, 1659-1664.
- _____, ROGER, G., MAUREL-PALACIN, D., MARCOUX, E. & LAROUSSI, A. (1995): Chemistry of some Pb - (Cu,Fe) - (Sb,Bi) sulfosalts from France and Portugal. Implications for the crystal chemistry of lead sulfosalts in the Cu-poor part of the $Pb_2S_2 - Cu_2S - Sb_2S_3 - Bi_2S_3$ system. *Mineral. Petrol.* **53**, 229-250.
- MOZGOVA, N.N., NENASHEVA, S.N., BORODAEV, YU.S. & YUDOVSKAYA, M.A. (1994): Nuffieldite from the Maleevskoe massive sulfide deposit, Russia. *Can. Mineral.* **32**, 359-364.
- MUMME, W.G. (1975a): The crystal structure of krupkaite, $CuPbBi_3S_6$, from the Juno mine at Tennant Creek, Northern Territory, Australia. *Am. Mineral.* **60**, 300-308.
- _____ (1975b): Junoite, $Cu_2Pb_3Bi_8(S,Se)_{16}$, a new sulfosalts from Tennant Creek, Australia: its crystal structure and relationship with other bismuth sulfosalts. *Am. Mineral.* **60**, 548-558.
- _____ (1980): Weibullite, $Ag_{0.32}Pb_{5.09}Bi_{8.55}Se_{6.08}S_{11.92}$ from Falun, Sweden: a higher homologue of galenobismutite. *Can. Mineral.* **18**, 1-12.
- _____ & WATTS, J.A. (1976): Pekoite, $CuPbBi_1S_{18}$, a new member of the bismuthinite-aikinite mineral series: its crystal structure and relationship with naturally- and synthetically-formed members. *Can. Mineral.* **14**, 322-333.
- OHMASA, M. & NOWACKI, W. (1970): A redetermination of the crystal structure of aikinite $[Bi_2S_2]SiCu^{IV}Pb^{VII}]$. *Z. Kristallogr.* **132**, 71-86.
- PARISE, J.B. & SMITH, P.P.K. (1984): Structure of the tin antimony sulphide $Sn_6Sb_{10}S_{21}$. *Acta Crystallogr.* **C40**, 1772-1776.
- RODIER, N. (1973): Structure cristalline du sulfure mixte de thulium et de cérium $TmCeS_3$. *Bull. Soc. fr. Minéral. Cristallogr.* **96**, 350-355.
- SRIKRISHNAN, T. & NOWACKI, W. (1974): A redetermination of the crystal structure of cosalite, $Pb_2Bi_2S_5$. *Z. Kristallogr.* **140**, 114-136.
- TAKÉUCHI, Y. & HAGA, N. (1969): On the crystal structure of seligmannite, $PbCuAsS_3$ and related minerals. *Z. Kristallogr.* **130**, 254-260.
- WALKER, N. & STUART, D. (1983): An empirical method for correcting diffractometer data for absorption effects. *Acta Crystallogr.* **A39**, 158-166.
- WUENSCH, B.J. (1964): The crystal structure of tetrahedrite, $Cu_{12}Sb_4S_{13}$. *Z. Kristallogr.* **119**, 437-453.

Received October 16, 1996, revised manuscript accepted February 26, 1997.